JOURNAL OF Applied Polymer SCIENCE

Characterization of four different lignins as a first step toward the identification of suitable end-use applications

Farshad Oveissi, Pedram Fatehi
Chemical Engineering Department, Lakehead University, 955 Oliver Road, Thunder Bay, Ontario P7B 5E1, Canada
Correspondence to: P. Fatehi (E-mail: pfatehi@lakeheadu.ca)

ABSTRACT: To determine the most appropriate use of lignin, surface, structural, and thermal characteristics of lignin was investigated in this work. It was observed that kraft lignin (KL), the lignin of prehydrolysis liquor (LPHL), lignosulfonate of NSSC process (LSL), and lignosulfonates (LSs) of sulfite pulping process had 0.67, 0.25, 0.90, and 1.52–2.25 meq/g anionic charge density, and 6.3, 2.1, 10.1, and 8.8–10.1 nm hydrodynamic diameter, respectively. These results suggested that LSL and LSs could be used more effectively than other lignin as filler modifiers, flocculants, and dispersants. The combustion studies of the lignin samples suggested that KL and LPHL combusted more efficiently than other samples, as they had high heating (calorific) values of 27.02 and 19.2 MJ/kg, the apparent activation energy of 126.64 and 99.14 kJ/mol based on Flynn–Wall–Ozawa method and 122.16 and 94.73 kJ/mol based on Kissinger–Akahira–Sunose and no ash, respectively. © 2015 Wiley Periodicals, Inc. J. Appl. Polym. Sci. **2015**, *132*, 42336.

KEYWORDS: biopolymers and renewable polymers; kinetics; thermal properties

Received 24 January 2015; accepted 10 April 2015
DOI: 10.1002/app.42336

INTRODUCTION

Forest biorefinery is an alternative approach for revisiting traditional pulp and paper industry.[1–3] Forest biorefinery concept aims not only to reduce the production cost of energy but also to produce value-added products from lignocelluloses.[2] One scenario of biorefinery is to produce value-added products from lignin that is generated, but not utilized well in pulping processes. In this regard, various processes were proposed in order to isolate lignin from pulping spent liquors. In these processes, isolated lignin can be used as an energy source or in production of value-added products.[4–6]

In neutral sulfite semichemical (NSSC) pulping process, wood chips are treated with sodium sulfite and carbonate to soften the structure of wood chips prior to NSSC pulping. The spent liquor (SL) of this process contains a portion of lignocelluloses, which is currently wasted in the wastewater of the mill.[7,8] In the kraft-based dissolving pulp process, hemicelluloses and lignin are partially separated from wood chips and dissolved in prehydrolysis liquor (PHL) of the process. The PHL is mixed with black liquor and sent to the evaporators of the kraft pulping process prior to combustion, but as PHL is a dilute stream, it increases the load to the evaporators.[7–9]

Kraft lignin is already used as fuel in the kraft pulping process. Kraft lignin can be extracted from black liquor via Lignoboost and LignoForce™ technologies.[10,11] Both processes are commercially used in Sweden, USA, and Canada to extract kraft lignin from black liquor. In some kraft pulping processes, recovery boilers are bottlenecks. Therefore, the extraction of kraft lignin may 1) help increase the production capacity of the mills and 2) facilitate the production of kraft lignin-based value-added products. The extraction of lignosulfonates from NSSC spent liquors was assessed using ultrafiltration, adsorption, and flocculation processes; however, these processes have not been commercialized yet. Similarly, acidification, adsorption, and flocculation were proposed to extract lignin from prehydrolysis liquor, but they were laboratory scale studies.[1,4,5,9]

In the past, lignosulfonates were proposed to be used as adhesives,[12] plasticisers in concrete,[13] and dye dispersants.[14] Lignin was also proposed to be used in a variety of polymer applications such as lubricants, stabilizers,[15] surfactants,[16] epoxy resins,[17] and superabsorbent hydrogels.[18] The lignin of PHL was also used as a filler modifier,[9] and fuel source in the past.[1,2] Kraft lignin can be used in the production of carbon and composite fibers or used as fuel.[18,19] However, the most suitable applications of lignin generated from the SL of NSSC process and the PHL of kraft-based dissolving pulp process have not been identified yet.

Lignin has a three-dimensional structure with many aromatic and aliphatic groups, which makes its modification and end-use application challenging. In the literature, it was claimed that lignins have various functional groups (i.e., carboxylate and

sulfonate) depending on its type and origin.[12,20] However, no study was conducted on analyzing the chemical, thermal, and combustion behavior of lignin present in the spent liquors of PHL and NSSC processes. This study aims to characterize lignin separated from industrially produced SL of NSSC and PHL of and kraft-based dissolving pulp processes, and to compare their properties with those of commercial lignosulfonates and kraft lignin. The surface, chemical, and thermal assessments of lignin are important parameters that affect the properties of end use lignin-based products.[21] The main novelty of this work is the surface, chemical, structural, and thermal analyses of various lignins to identify suitable end-use applications for them. As lignin is vastly produced in pulping processes in the world, the identification of a suitable end-use application for underutilized lignin will help their processes to be more financially profitable and environmentally friendly.

MATERIALS AND METHODS

Materials

Tego@trant A100, 1,3-didecyl-2-methylimidazolium (TEGO), was purchased from Metrohm (Canada) and used for the determination of carboxylate and sulfonate groups attached to lignin. Also, the solution (0.005 N) of polydiallyldimethylammonium chloride (PDADMAC) was purchased from Sigma–Aldrich and used as received to measure the total anionic charge density of lignin samples. Washed and dried hardwood kraft lignin (KL) was supplied by FPInnovations from its pilot facilities in Thunder Bay, ON.[22] Hardwood lignosulfonic acid sodium salt (LS1) was purchased from Sigma–Aldrich, while hardwood sodium lignosulfonate powder (LS2) was received from a Canadian company in Quebec province. The spent liquor (SL) of NSSC received from a mill located in New Brunswick, Canada. This mill did not have a recovery boiler. In this process, hardwood chips are treated at 180°C for 15–18 min using caustic and sulfite prior to refining in the NSSC pulping process. Wood chips from maple, poplar, and birch with the mass ratio of 7 : 2 : 1 are used in the kraft-based dissolving pulp production in a mill, located in New Brunswick, Canada.[23] The hemicelluloses and a part of lignin are separated in the pre-hydrolysis stage. The pre-hydrolysis liquor (PHL) of this process obtained from the aforementioned mill and used as received.

LPHL and LSL Collection

Both SL and PHL samples were initially centrifuged at 1000 rpm for 10 min using a Survall ST16 centrifuge to remove large particles (i.e., solid woody components). Afterwards, SL and PHL samples were acidified using 60 wt % sulfuric acid to a pH of 1.5 and kept for 60 min under stirring. For a commercial use of lignin, an alternative method should be developed to extract lignin from PHL and SL. Then, the samples were centrifuged at 2500 rpm for 10 min and the precipitates were collected. This treatment aimed to isolate the lignin from SL and PHL. The isolated lignin of SL (LSL), PHL (LPHL), LS1, and LS2 were oven dried at 60°C for a week and then used in this study.

Elemental and FTIR Analyses

Elemental (ultimate) analysis was performed on all dried lignin samples using a Vario EL cube instrument (Germany) according to the previously described method.[4,24] For this analysis, <50 mg of sample was used with two CAHN C-31 microblances (7 pt) associated with HR-2021 top loader 5 pt Fourier Transform Infrared Spectrophotometer (FTIR) and Tensor 37 (Bruker, Canada) was assessed for analyzing the functional groups associated with lignin samples. The FTIR spectra were developed by embedding <10 mg of sample on KBr disc. The resolution of spectroscopy was 2 cm^{-1} in a frequency range of 700–4000 cm^{-1}.

Sulfonate, Carboxylate Groups, and Total Charge Density Analyses

Initially, aqueous solutions (1 wt %) of lignin samples were made from dried samples and incubated in a C76 New Brunswick water bath shaker at pH 10.5, 30 C, and 100 rpm for 1 h. Then, 1–2 mL of lignin sample solutions were titrated against PDADMAC standard solution (0.005 M) using a Mütek PCD04 charge titrator (Herrsching, Germany), and the charge density of lignin samples were measured [eq. (1)].

$$\text{Charge Density}\left(\frac{\text{meq}}{\text{g}}\right) = \frac{\text{Volume of titrant} \times \text{concentration of titrant}}{\text{mass of lignin}} \quad (1)$$

To determine the amount of sulfonate group attached to lignin, 1 wt % aqueous solutions of lignin was prepared and incubated at pH 10, 30°C and 100 rpm for 1 h in a C76 New Brunswick water bath. Afterwards, all solutions were titrated against TEGO (0.004 mol/L) using a Metrohm 905 Titrando (Canada). The sulfonate group attached to lignin was determined according to eq. (2):

$$\text{Sulfonate group content}\left(\frac{\text{meq}}{\text{g}}\right) = \frac{\text{Volume of Point of inflection} \times \text{Tego concentration}}{\text{mass of lignin}} \quad (2)$$

To measure the amount of carboxylate group attached to lignin, the same protocol was followed, but at pH 10. Consequently, the carboxylate group content was measured based on eq. (3):

$$\text{Carboxylate group content}\left(\frac{\text{meq}}{\text{g}}\right) = \frac{\text{Volume of Point inflection} \times \text{Tego concentration}}{\text{mass of lignin}} - \text{the sulfonate group content} \quad (3)$$

All measurements were conducted three times and the averages of the three were reported.

Hydrodynamic Diameter Analysis

The molecular diameter of all lignin samples was measured by a dynamic light scattering (DLS) (Brookhaven BI200, USA) at 90° according to the method described in the literature.[25] Alkaline aqueous solutions of 1 wt % of lignin samples were prepared at pH 10 (using NaOH) and room temperature. A scattering angle of 90° was applied for reading the hydrodynamic diameter of lignin fragments in solutions. Based on volume, the results were reported as the average and the standard deviation for more

than five measurements was reported. pH 10 was selected for this measurement as KL is soluble at a pH of higher than 10.

Calorific Value and Thermogravimetric Analysis

Calorific value or high heating value (HHV) of lignin samples was measured according to ASTM E711-87 using a Parr 6200 oxygen bomb calorimeter as previously described.[7] Thermogravimetric analysis (TGA) was assessed for all oven dried samples by a thermogravimetric analyzer (TGA)-i1000 series (Instrument Specialist Inc., U.S.A.) in air at 35 mL/min and increment rates of 10, 12.5, 15, 17.5, and 20°C/min according to an establish method.[26]

Activation Energy Determination

Nonisothermal methods have been applied to calculate the effective activation energy as a function of conversion rather than temperature.[27] It was claimed that in nonisothermal solid-state kinetic studies, the rate of conversion of biomass to char and volatiles (tar and gas) would follow eq. (4):[27]

$$\frac{d\alpha}{dt} = k(T) \times f(\alpha) \tag{4}$$

in which $k(T)$ is the temperature dependent rate constant, $f(\alpha)$ is the temperature-independent function of conversion. $k(T)$ and α can be replaced by Arrhenius equation according to eqs. (5) and (6), respectively, in eq. (7):

$$k(T) = A.\exp\left(-\frac{E}{RT}\right) \tag{5}$$

$$\alpha = \frac{m_o - m_t}{m_o - m_\infty} \tag{6}$$

$$\frac{d\alpha}{dt} = A.\exp\left(-\frac{E}{RT}\right) f(\alpha) \tag{7}$$

where A, R, E, and α corresponded to frequency factor, the universal gas constant, activation energy, and sample conversion, respectively. Also, m_0, m_∞, and m_t are the mass of samples before and after the reaction and at time t, respectively. Equation (7) and the heating rate, β, can be combined to produce $G(\alpha)$, and then rearranged in two isoconversional methods developed by Flynn–Wall–Ozawa (FWO) (eq. (8)) and Kissinger–Akahira–Sunose (KAS) [eq. (9)]:[27,28]

$$\ln(\beta) = \ln\left[\frac{0.0084 \times A \times E}{R \times G(\alpha)}\right] - 1.0516\frac{E}{RT} \tag{8}$$

$$\ln\left(\frac{\beta}{T^2}\right) = \ln\left[\frac{A \times R}{E \times G(\alpha)}\right] - \frac{E}{RT} \tag{9}$$

Based on FWO and KAS methods, $\ln(\beta)$ versus $1/T$ and $\ln(\beta/T^2)$ versus $1/T$ would be straight lines at any constant α. Consequently, the slopes of these straight lines yield the apparent activation energy for the combustion of lignin samples.

RESULTS AND DISCUSSION

Structural Characterization

Figure 1 depicts the FTIR spectra of lignin samples. All samples had a peak at 3360 cm^{-1}; however, the intensity of this peak was greater in LPHL than other samples. This peak accounts for stretching of hydroxyl groups in lignin.[29] KL and LPHL had a peak at 1713 cm^{-1}, which corresponded to the carboxylate group in lignin.[30] This peak was hardly observable in LS1

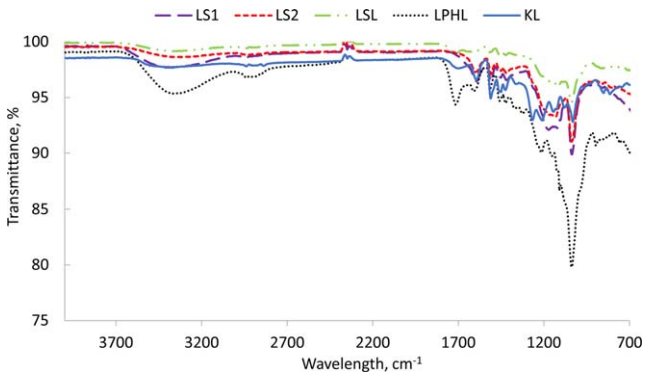

Figure 1. FTIR spectra of lignin samples. [Color figure can be viewed in the online issue, which is available at wileyonlinelibrary.com.]

implying that LS1 did not have a noticeable amount of carboxylate group. In the literature, it was stated that aromatic skeletal vibrations present at the wavelength range of 1400–1600 cm^{-1} in the FTIR spectrum.[20,31] It was claimed that the major peak of lignin mirrored at 1032 cm^{-1}.[32] This peak (1032–1034 cm^{-1}) is corresponded to the plane deformation of aromatic C—H in guaiacyl unit.[33,34] The peaks of sulfate groups were observed at 620–635 cm^{-1} and 1100–1137 cm^{-1} ranges.[20,31,35] Also, the decrease in LSL peak at 630 cm^{-1} was less than that in LS1 and LS2. From this analysis, it can be concluded that the sulfite content of KL and LPHL was less than that of others.

Charge Density and Hydrodynamic Diameter Characterization

It is well known that charge density plays a significant role in the adsorption of polymers on adsorbents and the flocculation of macromolecules in polyelectrolyte solutions.[36–38] Generally, the adsorption of lignocelluloses on adsorbents occur via developing mainly hydrogen bonding, and thus the amount of anionic charged groups (i.e., carboxylate and sulfonate groups) attached to lignocelluloses is critical.[5,39] Furthermore, lignocelluloses bond with other dissolved materials in polyelectrolyte solutions via developing hydrogen bonding and electrostatic forces.[40] In this case, the charged groups of lignocelluloses will attract or repel the charged groups of other constituents in the solutions and hence form flocs or disperse dissolved materials in solutions.[41] Thus, determining the charge density of lignin is critical for evaluating its adsorption/flocculation performance. In this regard, the charge density of lignin samples was measured and listed in Table I. The overall charge density of all samples was negative. It is evident that the anionic charge density of LS2 (2.25 meq/g) and LS1 (1.52 meq/g) were more than that of LSL (0.9 meq/g), KL (0.67 meq/g), and LPHL (0.25 meq/g). In the literature, it was stated that the anionic charge density of lignin was mainly attributed to sulfonate and carboxylate groups.[5,42] The sulfonate and carboxylate groups of all samples were measured and listed in Table I. As can be seen, 88% of anionic charge density of LPHL was related to carboxylate group and only 4% of that corresponded to sulfonate group. The shares of sulfonate group in total charge density were 0, 87, 85, and 78% and the shares of carboxylate group were 81, 7, 10, and 16% in KL, LS1, LS2, and LSL, respectively.

Table I. Surface Charge Density and Hydrodynamic Diameter of Lignin

Sample ID	Anionic charge density, meq/g	Sulfonate group, meq/g	Carboxylate group, meq/g	Hydrodynamic diameter, nm
LPHL	0.25 ± 0.01	0.01 ± 0.00	0.22 ± 0.01	2.1 ± 0.2
LSL	0.90 ± 0.03	0.70 ± 0.01	0.14 ± 0.02	10.1 ± 1.1
LS1	1.52 ± 0.02	1.33 ± 0.02	0.11 ± 0.01	10.1 ± 0.9
LS2	2.25 ± 0.01	1.92 ± 0.02	0.23 ± 0.02	8.8 ± 1.2
KL	0.67 ± 0.02	0.00 ± 0.00	0.54 ± 0.03	6.3 ± 0.7

In the literature, the carboxylate group content of various softwood lignin samples obtained from LignoBoost process was 0.3–0.58 mmol/g (via ^{31}P-NMR), which is in harmony with the results obtained in this study.[43] It should be noted that based on the present technology of prehydrolysis process practiced at the mill, PHL is mixed with black liquor that is produced in the previous batch of kraft pulping at a high temperature and thus it was not possible to obtain PHL with no absolute black liquor contaminations. The sulfonate content of PHL lignin might be due to the formation of sulfonate group on lignin during this mixing process. The sulfonation of lignin under alkaline conditions and a high temperature was reported in the past.[44,45]Also, it should be highlighted that the sulfonate and carboxylate groups and total charge density of LS2 were higher than those of other samples. These results are in harmony with observed peaks of carboxylate and sulfonate groups in FTIR analysis. Table I also lists the hydrodynamic diameter of lignin samples in 1 wt % water solution at pH 10 and room temperature. As can be seen, the diameters of LSL and LS1 were the same (10.1 nm) but higher than that of LS2, KL, and LPHL. In the literature, it was claimed that commercial sodium lignosulfonate (obtained from Chemische Werke Zell-Wildshausen, Düsseldorf, Germany) had the hydrodynamic diameter of 5–6 nm.[46] The hydrodynamic diameter is correlated to molecular weight of lignin samples. As lignin has a similar subunit structure, the larger the hydrodynamic diameter, the larger the molecular weight of lignin would be. The results showed that the smallest lignin sample was LPHL. The size of lignin plays a significant role on its adsorption and flocculation performance. It was stated that small polymers would diffuse more than large ones into pores of an adsorbent.[47] Therefore, if used as a surface modifier for a filler (i.e., adsorbent), more of small polymers will be diffused into the filler structure and thus its surface modifying performance will be deteriorated.[9] Instead, more of large polymers will adsorb on the surface of filler and modify its surface properties.[48] In this regard, at the same dosage, LPHL would not be suitable as a surface modifier as it is the smallest, and LSL and LS1 would work more effectively on modifying the surface properties of fillers. In addition, it was claimed that the smaller the polymers, the smaller the flocs would be formed.[1] Hence, via interacting with a specific particle in a solution, LPHL or KL would form smaller flocs than would LSL, LS1, or LS2 in solutions. Therefore, LS samples would be more effective flocculant than LPHL and KL. It is also well known that polymers with large hydrodynamic diameter have stronger steric hindrance, which results in higher dispersion.[49] Consequently, LSL, LS1, and LS2 could be better dispersants than LHPL and KL.[50,51]

CHNSO and HHV Analyses

Table II lists the elemental analysis of lignin samples. As can be seen, KL and LPHL had less sulfur content than other lignin samples. Also, the inorganic content (i.e., other elements) of KL and LPHL were the least in comparison with that of other samples. The remaining elements that were not reported in this study were usually the residual of cooking/pulping chemicals and inorganics originated from wood. Table II also lists the HHV of lignin samples. It is evident that KL generated more energy (HHV of 27.02 MJ/kg) than other tested samples ($HHV_{KL} > HHV_{LPHL} > HHV_{LS2} > HHV_{LS1} > HHV_{LSL}$). One study reported that the lignosulfonate obtained from hydrolyzate of pine wood had an HHV of 25 MJ/kg.[52] In another study, it was reported that alkali lignin had an HHV of 19 MJ/kg.[53] It was claimed that HHV of an organic materials is a function of its organic elements (ultimate).[54–56] A recent study on lignin of black liquor showed that HHV can be predicted based on the carbon content of lignin (eq. (10)).[57]

$$HHV_{model} = 0.40659 \times X_c \quad (10)$$

where X_c is the carbon content (wt %) of the sample. Based on eq. (10), HHV_{model} of KL, LPHL, LSL, LS1, and LS2 were

Table II. CHNSO and High Heating Value (HHV) of Lignin

Sample ID	*N* (wt %)	*C* (wt %)	*H* (wt %)	*S* (wt %)	*O* (wt %)	Other elements (wt %)	$HHV_{measured}$ (MJ/ kg)	HHV_{model} (MJ/ kg)
LPHL	0.14	43.58	5.49	2.62	48.09	0.09	19.20	17.72
LSL	0.43	36.30	4.49	7.65	46.90	4.23	16.03	14.76
LS1	0.22	41.15	4.70	5.32	43.21	5.41	17.92	16.73
LS2	0.86	41.33	4.65	6.06	39.64	7.47	18.45	16.80
KL	0.06	63.07	5.97	0.23	30.60	0.07	27.02	25.64

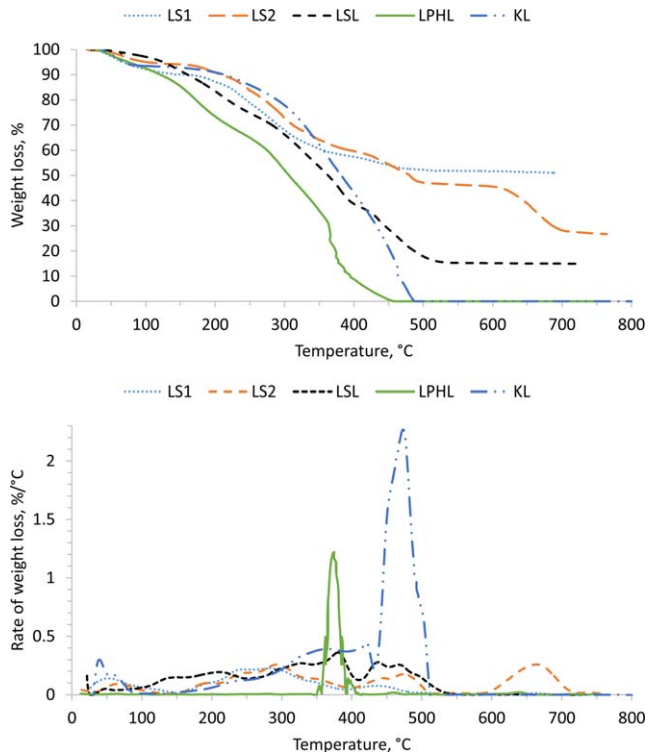

Figure 2. Weight loss (top) and weight loss rate (bottom) of LS1, LS2, LSL, LPHL, and KL (conducted in air at 35 mL/min and heating rate of 10°C/min). [Color figure can be viewed in the online issue, which is available at wileyonlinelibrary.com.]

calculated and tabulated in Table II. A comparison between the calculated and measured values revealed 7–9% difference (i.e., error).

TGA Analysis

TGA analysis not only helps understand the thermal behavior of lignin as fuel but also indicates how lignin can behave under different thermal treatments in composites. The weight loss and the rate of weight loss of lignin samples versus temperature in air (35 mL/min) and combustion rate of 10°C/min are depicted in Figure 2. It is apparent that the thermal decomposition of lignin occurred at different temperatures due to the heterogeneous and complex structure of lignin.[58] Volatile components would also be generated during the combustion of lignin, which mirrored in several peaks in Figure 2.[58] It is evident that KL and LPHL showed less resistance to combustion than other samples. By burning the samples to 700°C, 15 wt % of LSL, 51 wt % of LS1, and 27 wt % of LS2 were remained. Interestingly, all of LPHL and KL were combusted and no ash was remained at 700°C. The peaks below 150°C were due to the evaporation of moisture content of lignin samples.[59] It is evident that a part of LSL decomposed at 214°C (T_{p1}). This degradation may be due to the removal of terminal groups of LSL[60] or probably the degradation of lignin–hemicellulose complexes accompanied in LSL.[59] Figure 2 also shows that the maximum combustion of KL and LPHL occurred at 469 and 375°C, which corresponded to 6 and 19% of remaining weight, respectively. This peak (T_{p2}) was observed at 383°C in LSL, 297°C in LS1, and 299°C in LS2, which were related to 43, 71, and 73% of weight loss, respectively. In the literature, it was stated that the maximum degradation of lignin occurred at 330–400°C.[59] In all samples (except LPHL), the second major increase in the rate of weight loss (T_{p3}) occurred at the temperature range of 439–479°C, which might be due to the conversion of lignin to phenols.[60] In this peak, the remaining mass of LS1, LS2, and LSL were 54.8, 50.4, and 24.3 wt %, respectively. Moreover, a portion of LS2 decomposed at 657°C (T_{P4}), which may correspond to the degradation of phenols to carbonaceous structure.[60,61]

Table III summarized the combustion parameters of lignin, which were obtained from Figure 2. Reactivity index was defined as the maximum rate in which the biomass or char combusted in oxidizing or reducing atmosphere[62]

$$R = \frac{1}{w_o} \times \left(\frac{dw}{dt}\right)_{max} \quad (11)$$

where w_0 is the initial mass of sample (kg) and $\left(\frac{dw}{dt}\right)_{max}$ is the maximum rate of weight loss (%/s). Reactivity indices were calculated based on the combustion rate and listed in Table III. It should be highlighted that a greater R represents a higher reactivity describing that constituents of biomass or char volatizes easier by the gasifying agent.[62,63] As can be seen, KL and LPHL had the highest reactivity indices of 51,758 and 22,222% kg^{-1} s^{-1}, respectively, while other samples had the reactivity index of 5,000–7,000% kg^{-1} s^{-1}. In the literature, it was stated that olive waste had a reactivity index of 23,807% kg^{-1} s^{-1}.[57] In other words, KL and LPHL reacts faster with the gasifying agent (air) than other samples. It can be concluded that KL and LPHL combusted more efficiently than other lignin samples.

Table III. Properties of Combustion of Lignin Obtained from Figure 2

	T_P (°C)						
Lignin	T_{P1}	T_{P2}	T_{P3}	T_{P4}	DTG_{max} (%/°C)	W_R (%)	R (% kg^{-1} s^{-1})
LPHL	-	374.7	-	-	1.200	0.00	22,222
LSL	214.2	382.9	467.9	-	0.357	14.95	7256
LS1	-	296.8	439.1	-	0.225	51.03	5000
LS2	-	299.2	478.6	665.6	0.259	26.70	6167
KL	-	469.1	-	-	2.267	0.00	51,758

T_P: peak temperature.
DTG_{max}: maximum rate of weight loss.
W_R: residual mass.

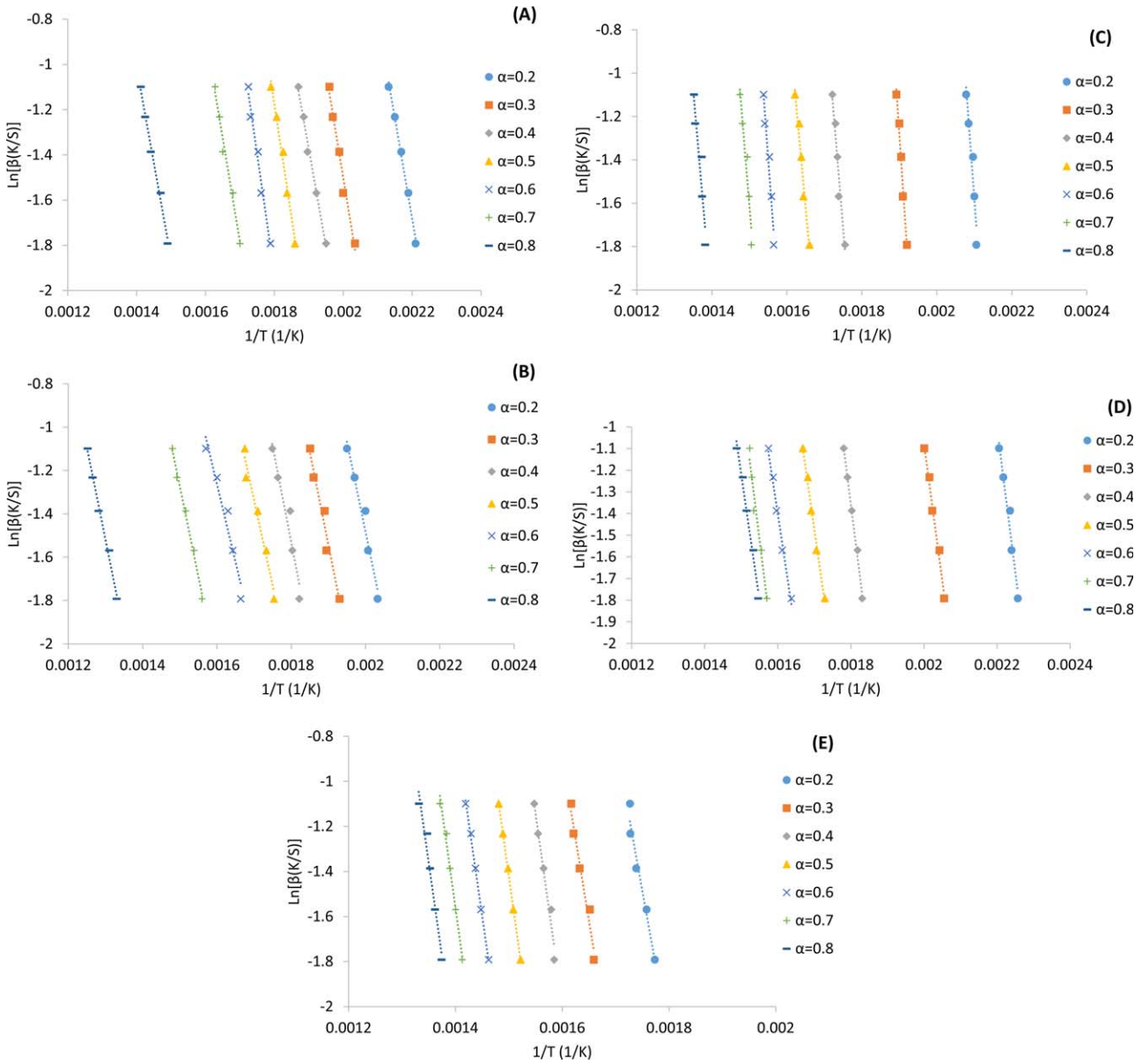

Figure 3. Determination of activation energy of (A) LS1, (B) LS2, (C) LSL, (D) LPHL, and (E) KL at different α values using FWO method. [Color figure can be viewed in the online issue, which is available at wileyonlinelibrary.com.]

Kinetic Analysis

To comprehend a detailed understanding of combustion behavior of lignin samples, Flynn–Wall–Ozawa (FWO) and Kissinger–Akahira–Sunose (KAS) nonisothermal methods were applied on thermogravimetric data obtained in Figure 2. The apparent activation energy (E) was calculated by plotting $\ln(\beta)$ vs $1/T$ (FWO method) and $\ln(\beta/T^2)$ vs $1/T$ (KAS method) at various sample conversions (α) based on eqs. (8) and (9). As stated earlier, the heating rates (β) of 10, 12.5, 15, 17.5, and 20°C/min were used to evaluate the activation energy of samples under air (35 mL/min). Figures 3 and 4 correspond to FWO and KAS analyses, respectively. It is evident that the slopes of fitted lines were similar in each sample, but were not the same in all conversions (α). The variation in slopes at conversion ratios may be due to the complexity and multistep reactions of lignin to char during the combustion.[27]

Table IV lists the calculated activation energy (the energy required for breaking lignin molecules to start combusting) in all α (conversion of lignin to char and volatiles) values via FWO and KAS methods. The average value of E was reported for each sample as an apparent activation energy. As can be seen, the highest apparent activation energies were achieved for LSL, which were 173.98 (FWO) and 172.89 (KAS) kJ/mol. Also, the apparent activation energies of 126.64 (FWO) and 122.16 (KAS) kJ/mol for KL, 99.14 (FWO) and 94.73 (KAS) kJ/mol for LPHL, 73.49 (FWO) and 68.03 (KAS) kJ/mol for LS1, and 65.17 (FWO) and 58.49 (KAS) kJ/mol for LS2 were obtained,

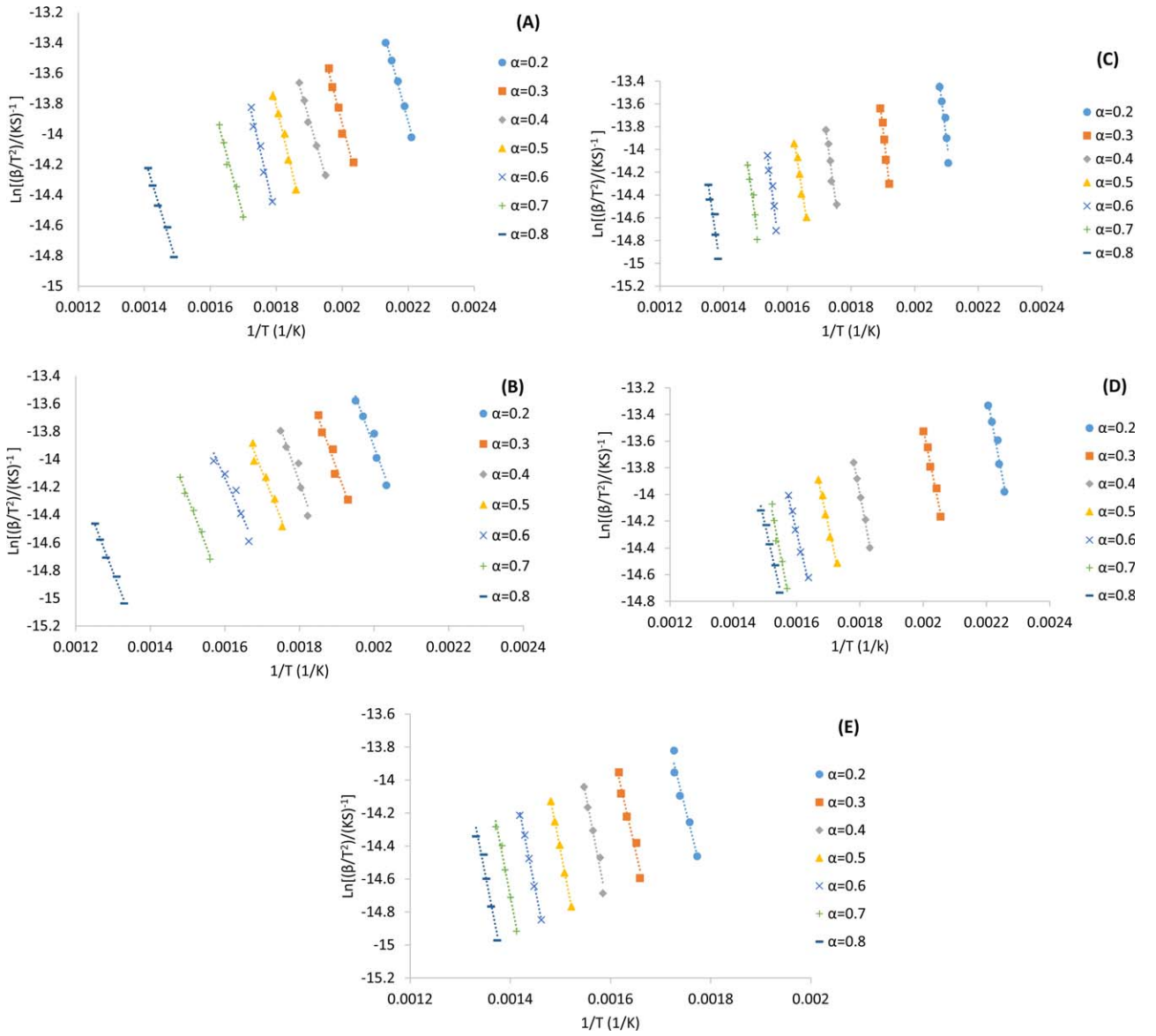

Figure 4. Determination of activation energy of (A) LS1, (B) LS2, (C) LSL, (D) LPHL, and (E) KL at different α values using KAS method. [Color figure can be viewed in the online issue, which is available at wileyonlinelibrary.com.]

respectively. It was previously reported that lignin extracted from spruce sawdust had the activation energy (based on Arrhenius equation without the temperature integral) of 13–19 kcal/mol (≈ 54–79.5 kJ/mol).[64] It should be highlighted that the Arrhenius equation (without the temperature integral) is insufficiently accurate for complex condensed phase systems of thermal analysis.[65]

In another study, the apparent activation energy for poplar was reported to be in the range of 107.86–209.49 kJ/mol and 104.95–209.90 kJ/mol for FWO and KAS, respectively.[27] This comparison implies that the values of activation energies were significantly different among various studies. In other words, the apparent activation energy for the combustion of lignin is a function of lignin origin and probably structure. Consequently, LSL needs more energy than other samples to start the combustion. It should be highlighted that LPHL required less energy than KL to start burning.

Consequently, the TGA analysis confirmed low thermal resistance and ash content of LHPL and KL. Also, LPHL and KL had better combustion efficiency than other samples with HHV of 27.02 and 19.2 MJ/kg, and reactivity indices of 51758 and

Table IV. Average of Activation Energy (kJ/mol) Calculated Based on FWO and KAS Methods for Different α Values Obtained from Figures 3 and 4 for the Combustion of Lignins in Air

Sample	FWO method	KAS method
LPHL	99.14	94.73
LSL	173.98	172.89
LS1	73.49	68.03
LS2	65.17	58.49
KL	126.64	122.16

22222 % kg^{-1} s^{-1}, respectively. In addition, the apparent activation energy of 126.64, 99.14, 173.98, 73.49, and 65.17 kJ/mol through FWO method and 122.16, 94.73, 172.89, 68.03, and 58.49 kJ/mol via KAS method were obtained for KL, LPHL, LSL, LS1, and LS2, respectively. These results may suggest that LPHL would be a suitable fuel source after KL.

CONCLUSIONS

KL, LPHL, LSL, LS1, and LS2 had 0.67, 0.25, 0.90, and 1.25–1.52 meq/g anionic charge densities; 0.54, 0.22, 0.14, and 0.11–0.23 meq/g carboxylate group; and 0, 0.01, 0.70, and 1.33–1.92 meq/g sulfonate group, respectively. The results also indicated that LSL and LS1 had the same hydrodynamic diameter (10.1 nm), which was higher than that of KL, LPHL, and LS2. The hydrodynamic diameter and charge density analyses confirmed that lignosulfonates (LSL, LS1, and LS2) were more appropriate to be used as a filler modifier, flocculants, and dispersants. The TGA analysis confirmed low thermal resistance and ash content of LHPL and KL. The results also indicated that LPHL had better combustion efficiency than other samples with HHV of 27.02 and 19.2 MJ/kg, and reactivity indices of 51758 and 22222 % kg^{-1} s^{-1}, respectively. In addition, the apparent activation energy of 126.64, 99.14, 173.98, 73.49, and 65.17 kJ/mol through FWO method and 122.16, 94.73, 172.89, 68.03, and 58.49 kJ/mol via KAS method were obtained for KL, LPHL, LSL, LS1, and LS2, respectively. These results may suggest that LPHL would be a suitable fuel source after KL.

ACKNOWLEDGMENTS

The authors declare no competing financial interest. This research was supported by NSERC Discovery grant and Canada Research Chair program.

REFERENCES

1. Saeed, A.; Fatehi, P.; Ni, Y. *Carbohydr. Polym.* **2011**, *86*, 1630.
2. Van Heiningen, A. *Pulp Pap. Canada* **2006**, *107*, 38.
3. Dansereau, L. P.; El-Halwagi, M.; Mansoornejad, B.; Stuart, P. *Comput. Chem. Eng.* **2014**, *63*, 34.
4. Oveissi, F.; Fatehi, P. *Env. Technol.* **2014**, *35*, 2597.
5. Liu, X.; Fatehi, P.; Ni, Y. *Ind. Eng. Chem. Res.* **2011**, *50*, 11706.
6. Holmqvist, A.; Wallberg, O.; Jönsson, A. S. *Chem. Eng. Res. Des.* **2005**, *83*, 994.
7. Dashtban, M.; Gilbert, A.; Fatehi, P. *Bioresour. Technol.* **2014**, *159*, 373.
8. Sitter, T.; Oveissi, F.; Fatehi, P. *J. Biotechnol.* **2014**, *173*, 19.
9. Fatehi, P.; Hamdan, F. C.; Ni, Y. *Carbohydr. Polym.* **2013**, *94*, 531.
10. Tomani, P. *Cellulose Chem. Technol.* **2010**, *44*, 53.
11. Kousini, L.; Holt-Hindle, P.; Maki, K.; Paleologou, M. *J. Sci. Technol.* **2012**, *2*, 6.
12. El Mansouri, N. E.; Salvadó, J. *Ind. Crops Prod.* **2006**, *24*, 8.
13. Pelisser, F.; Zavarise, N.; Longo, T. A.; Bernardin, A. M. *J. Cleaner Prod.* **2011**, *19*, 757.
14. Yang, D.; Li, H.; Qin, Y.; Zhong, R.; Bai, M.; Qiu, X. *J. Dispersion Sci. Technol.* **2014**, *36*, 532.
15. Kumar, S.; Mohanty, A.; Erickson, L.; Misra, M. *J. Biobased Mater. Bioenergy* **2009**, *3*, 1.
16. Olsen, S. N.; Bohlin, C.; Murphy, L.; Borch, K.; Mcfarland, K.; Sweeny, M.; Westh, P. *Enzyme Microb. Technol.* **2011**, *49*, 353.
17. Sasaki, C.; Wanaka, M.; Takagi, H.; Tamura, S.; Asada, C.; Nakamura, Y. *Ind. Crops Prod.* **2013**, *43*, 757.
18. Thakur, V. K.; Thakur, M. K.; Raghavan, P.; Kessler, M. R. *ACS Sustainable Chem. Eng.* **2014**, *2*, 1072.
19. Kadla, J.; Kubo, S.; Venditti, R.; Gilbert, R.; Compere, A.; Griffith, W. *Carbon* **2002**, *40*, 2913.
20. El Mansouri, N. E.; Salvadó, J. *Ind. Crops Prod.* **2007**, *26*, 116.
21. Lora, J. H.; Glasser, W. G. *J. Polym. Env.* **2002**, *10*, 39.
22. Maki, K.; Kousini, L.; Paleologou, M.; Haolt-Hindle, P. 2012 TAPPI PEERS Conference, USA, **2012**, 1863.
23. Saeed, A.; Jahan, M. S.; Li, H.; Liu, Z.; Ni, Y.; Van Heiningen, A. *Biomass Bioener.* **2012**, *39*, 14.
24. Fadeeva, V.; Tikhova, V.; Nikulicheva, O. *J. Anal. Chem.* **2008**, *63*, 1094.
25. Li, W.; Wang, Q.; Cui, S.; Huang, X.; Kakuda, Y. *Food Hydrocolloids* **2006**, *20*, 361.
26. Zhang, J.; Feng, L.; Wang, D.; Zhang, R.; Liu, G.; Cheng, G. *Bioresour. Technol.* **2014**, *153*, 379.
27. Slopiecka, K.; Bartocci, P.; Fantozzi, F. *Appl. Energy* **2012**, *97*, 491.
28. Li, D.; Chen, L.; Chen, S.; Zhang, X.; Chen, F.; Ye, N. *Fuel* **2012**, *96*, 185.
29. Laurichesse, S.; Avérous, L. *Polym.* **2013**, *54*, 3882.
30. Ishida, Y.; Sun, A. C.; Jikei, M.; Kakimoto, M. A. *Macromolecules* **2000**, *33*, 2832.
31. Maria, S. F.; Russell, L. M.; Turpin, B. J.; Porcja, R. J. *Atmos. Env.* **2002**, *36*, 5185.
32. Tucker, M. P.; Nguyen, Q. A.; Eddy, F. P.; Kadam, K. L.; Gedvilas, L. M.; Webb, J. D. *Appl. Biochem. Biotechnol.* **2001**, *91*, 51.
33. El Hage, R.; Brosse, N.; Chrusciel, L.; Sanchez, C.; Sannigrahi, P.; Ragauskas, A. *Polym. Degrad. Stab.* **2009**, *94*, 1632.
34. Xu, F.; Geng, Z.; Liu, C.; Ren, J.; Sun, J.; Sun, R. *J. Appl. Polym. Sci.* **2008**, *109*, 555.
35. Paul, K. W.; Borda, M. J.; Kubicki, J. D.; Sparks, D. L. *Langmuir* **2005**, *21*, 11071.
36. Zavgorodnya, O.; Serpe, M. J. *Colloid Polym. Sci.* **2011**, *289*, 591.
37. Barany, S.; Meszaros, R.; Marcinova, L.; Skvarla, J. *Colloids Surf A. Phisichochem. Eng. Aspets* **2011**, *383*, 48.
38. Gregory, J.; Barany, S. *Adv. Colloid Interface Sci.* **2011**, *169*, 1.
39. Nakagame, S.; Chandra, R. P.; Kadla, J. F.; Saddler, J. N. *Biotechnol. Bioeng.* **2011**, *108*, 538.

40. Yasarla, L. R.; Ramarao, B. V. *J. Biobased Mater. Bioenergy* **2013**, *7*, 684.
41. Nasser, M.; James, A. *Sep. Purif. Technol.* **2006**, *52*, 241.
42. Liu, X.; Fatehi, P.; Ni, Y. *Bioresour. Technol.* **2012**, *116*, 492.
43. Bylin, S.; Wells, T.; Sun, Q.; Ragauskas, A.; Theliander, H. *BioResour.* **2014**, *9*, 6002.
44. Gierer, J.; Lenz, B.; Wallin, N. H. *Acta Chemica Scandinavica* **1964**, 18.
45. Gierer, J.; Petterson, I. *Can. J. Chem.* **1977**, *55*, 593.
46. Tiemeyer, C.; Lange, A.; Plank, J. *Colloids Surf A: Physicochem. Eng. Aspects* **2014**, *456*, 139.
47. Bjelopavlic, M.; Newcombe, G.; Hayes, R. *J. Colloid Interface Sci.* **1999**, *210*, 271.
48. Huang, X.; Shen, J.; Qian, X. *Carbohydr. Polym.* **2013**, *98*, 931.
49. Ran, Q.; Somasundaran, P.; Miao, C.; Liu, J.; Wu, S.; Shen, J. *J. Colloid Interface Sci.* **2009**, *336*, 624.
50. Wei, R.; Peng, Y.; Seaman, D. *Miner. Eng.* **2013**, *50*, 93.
51. Xiao, S.; Tan, Y.; Xu, J.; Xiong, C.; Wang, X.; Su, S. *Appl. Clay Sci.* **2014**, *97-98*, 91.
52. Retsina, T.; Pylkkanen, V. U.S. Patent Application **2008**, *12/234*, 286.
53. Bu, Q.; Lei, H.; Wang, L.; Wei, Y.; Zhu, Y.; Zhang, X.; Liu, Y.; Yadavalli, G.; Tang, J. *Bioresour. Technol.* **2014**, *162*, 142.
54. Demirbas, A. *Energy Sourc.* **2003**, *25*, 629.
55. Sheng, C.; Azevedo, J. *Biomass Bioener.* **2005**, *28*, 499.
56. Vargas-Moreno, J.; Callejón-Ferre, A.; Pérez-Alonso, J.; Velázquez-Martí, B. A. *Renewab. Sustainab. Energy Rev.* **2012**, *16*, 3065.
57. Jablonský, M.; Ház, A.; Orságová, A.; Botková, M.; Šmatko, L.; Kočiš, J. Relationships Between Elemental Carbon Contents And Heating Values Of Lignins. 4th International Conference Renewable Energy Sources **2013**.
58. Lemes, A.; Soto-Oviedo, M.; Waldman, W.; Innocentini-Mei, L.; Durán, N. *J. Polym. Env.* **2010**, *18*, 250.
59. Singh, R.; Singh, S.; Trimukhe, K.; Pandare, K.; Bastawade, K.; Gokhale, D.; Varma, A. *Carbohydr. Polym.* **2005**, *62*, 57.
60. Wang, M.; Leitch, M.; Xu, C. *Eur. Polym. J.* **2009**, *45*, 3380.
61. Chen, Y.; Chen, Z.; Xiao, S.; Liu, H. *Thermochim. Acta* **2008**, *476*, 39.
62. Gomes, M. D. L. I.; Osório, E.; Vilela, A. C. F. *Mater. Res.* **2006**, *9*, 91.
63. Gil, M.; Riaza, J.; Álvarez, L.; Pevida, C.; Pis, J.; Rubiera, F. A. *J. Therm. Anal. Calorim.* **2012**, *109*, 49.
64. Ramiah, M. *J. Appl. Polym. Sci.* **1970**, *14*, 1323.
65. Flynn, J. H. *Thermochim. Acta* **1997**, *300*, 83.